Check for updates

OPEN

Unsupervised Quantum Gate Control for Gate-Model Quantum Computers

Laszlo Gyongyosi[1,2,3]

In near-term quantum computers, the operations are realized by unitary quantum gates. The precise and stable working mechanism of quantum gates is essential for the implementation of any complex quantum computations. Here, we define a method for the unsupervised control of quantum gates in near-term quantum computers. We model a scenario in which a tensor product structure of non-stable quantum gates is not controllable in terms of control theory. We prove that the non-stable quantum gate becomes controllable via a machine learning method if the quantum gates formulate an entangled gate structure.

Quantum computers[1–12] utilize quantum mechanics to solve computational problems more efficiently than traditional computers[1,3,4,13–46]. The experimental realizations of quantum computers have already begun to be implemented[1–4,8,9] to demonstrate the quantum supremacy[3,4] (advantages) of quantum computations[2,5–7,47]. In a gate-model quantum computer, the operations are performed by quantum gates (unitary operators)[13–15,18,20,32–36,39]. The precise and stable working mechanism of quantum gates is essential for the realization of any complex quantum computations. In particular, the quantum gates can communicate through a quantum bus[39,48–51] that consists of the quantum systems outputted by the quantum gates, along with several auxiliary quantum systems and measurement operators. The aim of the quantum bus is analogous to that of traditional communication buses, though in a quantum computer, the quantum bus can also entangle the quantum gates. Practically, the creation of the entangled gate structure is achievable by an appropriate measurement operator applied to the auxiliary systems on the quantum bus, where the auxiliary systems are correlated with the gate outputs. Here, we are focusing on the problem of controlling non-stable quantum gates in an entangled gate structure in gate-model quantum computers. Another important aspect is the application of gate-model quantum computations[24–31,52–55] in the near-term quantum devices of the quantum Internet[20,52,56–105] (such as in quantum repeaters[56–58,106–114], or in small scale quantum devices of the quantum Internet[20,56–58,65,66]).

Machine learning is about statistical inference of measured data. The aim of machine learning is to derive system models and effective control functions from noisy data (measurements)[24,115–117]. The field of machine learning is at the intersection of computer science, mathematics, artificial intelligence, and statistical sciences. Machine learning–based solutions have been applied successfully in academic and industrial studies as well as technology and marketing applications[24,115–117]. This has been possible mainly because the large amounts of data required by machine learning methods are now available due to the technical advancements in current telecommunication networks and data processing tools. The motivation behind the application of machine learning–based models for controlling complex physical systems[24,25,53,115,118–124]. is that these models can extract precise system models and optimal control functions in scenarios in which this task is hard or impossible by other control methods[24,33,53,115–117]. In a general architecture of machine learning–based controlling, the system model consists of a complex physical system subject to controlling, noisy measurement results from the physical system, a cost function, and the machine learning control unit, which outputs a control function to calibrate the physical system[24,115–117]. The machine learning unit uses the noisy measurements and the cost function as feedback information, formulating a learning loop. The aim of a machine learning–based control is to find an optimal control function that minimizes the cost function for the system calibration.

Here we define a framework for controlling entangled quantum gates in quantum computer architectures via unsupervised learning. In the system model, the quantum gates output quantum systems to a quantum bus that

¹School of Electronics and Computer Science, University of Southampton, Southampton, SO17 1BJ, UK. ²Department of Networked Systems and Services, Budapest University of Technology and Economics, Budapest, H-1117, Hungary. ³MTA-BME Information Systems Research Group, Hungarian Academy of Sciences, Budapest, H-1051, Hungary. e-mail: gyongyosi@hit.bme.hu

correlates these output quantum systems with some auxiliary quantum system (probe beams[39,48–51]). These auxiliary systems are then measured, providing information about the gate unitaries for the machine learning module. The quantum bus also contains a measurement operator to entangle the output quantum systems, which results in an entangled gate structure. In the control problem, it is assumed that a particular quantum gate oscillates randomly, i.e., a quantum gate is non-stable. We prove that this random oscillation is not controllable in terms of control theory[115–117] if the quantum gates formulate a product system (i.e., the quantum gates are unentangled). On the other hand, the non-stable quantum gate is controllable if the quantum gates are entangled. In this case, the randomly oscillating quantum gate can be controlled by a stable quantum gate in the joint gate structure. We also define a post-processing unit that processes the measurement results, which are then fed into the machine learning control ($\mathscr{C}$) unit to learn an optimal control function in an unsupervised manner. The $\mathscr{C}$ unit achieves the quantum gate calibration via the determination of an appropriate control function that minimizes a particular cost function defined for the mechanism. The output of the $\mathscr{C}$ block is a control parameter that achieves the calibration of the non-stable gate in the entangled gate structure. We also define a scheme for the calibration of the quantum bus states directly on the quantum bus. We provide the results for a particular gate pair in the entangled structure, but the results can be extended for an arbitrary setting with an arbitrary number of gates. The proposed framework provides an easily implementable and effective control mechanism for quantum gate structures. The results are particularly convenient for experimental quantum computers and the near-term quantum devices of the quantum Internet.

The novel contributions of our manuscript are as follows:

1. We prove that random oscillation of unitary quantum gates is not controllable in terms of control theory if the quantum gates formulate a product system. We show that the quantum gate becomes controllable if the quantum gates are entangled.
2. We show that for an entangled quantum gate structure, the randomly oscillating quantum gate can be controlled by a stable quantum gate in the entangled gate structure.
3. We define a post-processing unit that processes the measurement results, which are then fed into the machine learning unit to learn an optimal control function in an unsupervised manner.
4. The control achieves the quantum gate calibration via the determination of an appropriate control function that minimizes a particular cost function defined for the mechanism. The output of the control block is a control parameter that achieves the calibration of the non-stable gate in the entangled gate structure.
5. We define a scheme for the calibration of the quantum bus states directly on the quantum bus.
6. The proposed framework provides an effective control mechanism for entangled quantum gate structures. Since the results are independent from the level of scaling, the method is particularly convenient for experimental quantum computations and near-term quantum devices of the quantum Internet.

This paper is organized as follows. In Section 2, the related works are summarized. In Section 3, the system model is defined. Section 4 proposes the control problem. In Section 5, the control method is defined. Finally, Section 6 concludes the paper. Supplemental material is included in the Appendix.

Related works
The related works are as follows.

The theoretical background of the gate-model quantum computer environment utilized in our manuscript can be found in[13] and[14].

In[14], the authors studied the subject of objective function evaluation of computational problems fed into a gate-model quantum computer environment. The work focuses on a qubit architectures with a fixed hardware structure in the physical layout.

A scheme for the evaluation of objective function connectivity (computational pathway) in gate-model quantum computers has been proposed in[21]. Objective function examples can be found in[10,11]. A method for the optimization of the measurement procedure in gate-model quantum computers has been defined in[72]. An approach for the stabilization of the state of the quantum computer in an optimal state has been discussed in[74]. A framework for the design of quantum circuits for gate-model quantum computers has been defined in[75]. A method for the optimization of quantum memory units via quantum machine learning in near-term quantum devices has been defined in[67].

A control method of coupled spin dynamics and the design of NMR pulse sequences by gradient ascent algorithms has been conceived in[125].

An optimization algorithm related to gate-model quantum computer architectures is defined in[13]. In[126,127], the authors studied some relevant attributes of the algorithm. An application of the optimization algorithm to a bounded occurrence constraint problem can be found in[18].

In[40], the authors studied the objective function value distributions of the optimization algorithm. In[41–43], the authors analyzed the experimental implementation of the algorithm on near-term gate-model quantum devices.

An approximate approximation on a quantum annealer has been studied in[128]. In[129], the authors concealed approximate quantum adders with genetic algorithms, and analyzed the experimental scenarios. The proposed model employs a machine learning algorithm via genetic algorithms, for optimizing a quantum circuit in terms of the best gate sequence to be applied to achieve a certain global unitary operation.

In[15], the authors defined a gate-model quantum neural network model. A training method has been proposed in[73].

For a review on the noisy intermediate-scale quantum (NISQ) era, we suggest[1]. On the subject of quantum computational supremacy, see[4]. The complexity-theoretic foundations of quantum supremacy is studied in[3]. A survey on quantum channels can be found in[24], while for a survey on quantum computing, see[130].

Problem statement and system model

Problem statement.   The problems to be solved are given in Problems 1–4.

Problem 1 *Find a method to extract the gate unitary operations for the machine learning–based control of the quantum gates of the quantum computer.*

Problem 2 *Define a method to fix random oscillations of quantum gates in an entangled gate structure.*

Problem 3 *Find a P post-processing that yields the estimations of the unitary operations of the quantum gates in an arbitrary gate-model quantum computer.*

Problem 4 *Define a $\mathscr{C}$ unsupervised control method for the entangled gate structure of the quantum computer.*
The resolutions to Problems 1–4 are proposed in the Theorems and Lemmas.

System model.   The system model consist of n unitary gates, U_i, $i = 1, \ldots, n$, that output quantum states $|\varphi_i\rangle$, which are placed onto the Q_b quantum bus[39,48–51]. For simplicity, we assume qubit systems; therefore, the quantum systems are $d = 2$ dimensional, and Q_b is a qubus. In the Q_b qubus, for each $|\varphi_i\rangle$ an auxiliary qubit system $|0\rangle_i$ is associated via a CNOT gate. In a physical layer representation, the probe beam is a continuous quantum variable, i.e., a collection of a large number of photons implementable by laser or microwave pulses[39,48–51]). The CNOT gate refers to the interaction between the output states and the auxiliary systems.

To identify the correctness of the quantum gates, for each U_i, a reference angle $\pm\theta_i$ is associated in the phase space (i.e., the phase of $|0\rangle_i$ is rotated in the $\mathscr{S}$ phase space by an angle $\pm\theta_i$). The actual phase space angle of U_i is identified through the measurement of $|0\rangle_i$ via the M homodyne measurement[39,131]. The measurement results are post-processed by P post-processing unit and then fed into the $\mathscr{C}$ machine learning control block that achieves the calibration of the U_i quantum gates.

Finally, the system model contains an operator U_C for the direct correction of the actual $|\varphi_i\rangle$ states on Q_b and a second homodyne measurement M_b that creates entanglement between the calibrated states via the measurement of the $(n+1)$-th beam[39,131] $|0\rangle_b$.

The aim of the machine learning–based gate controlling procedure is to calibrate the working mechanism of the quantum operations via the derivation of a $C(\cdot)$ control function. The $C(\cdot)$ control function requires the construction of a system model by $\mathscr{C}$ from measurement information provided by an M measurement phase. The measurement information is post-processed via a P post-processing phase and are then fed into the $\mathscr{C}$ procedure to determine the optimal control function.

Without loss of generality, as vector M refers to the measurement results, then the output of $\mathscr{C}$ is defined as

$$\partial = C(P(M)), \tag{1}$$

where ∂ is the control parameter. The $s = P(M)$ system state is associated with a cost function f_s, while the ∂ control parameter is associated with a cost function f_∂. The functions f_s and f_∂ formulate the f_C cost function subject to a minimization as

$$f_C = f_s + \gamma f_\partial, \tag{2}$$

via the determination of an optimal control function $C^*(s)$ as

$$C^*(s) = \underset{\forall\, C(s)}{\arg\min} f_C(s). \tag{3}$$

Identify the unstable and stable gates.   The unstable and stable unitaries of the gate-model quantum computer can be identified via a homodyne measurement applied on the auxiliary quantum states of the quantum bus. The measurement extracts relevant information about the quantum gates to determine the stable and unstable unitaries. The method and results are given by Theorem 1.

Theorem 1 *(Identify the unstable and stable gates). The unitary operators of the n quantum gates U_i, $i = 1, \ldots, n$ of the quantum computer can be extracted via a M homodyne measurement of n auxiliary quantum systems $|0\rangle_i$ of Q_b.*

Proof. Let $|0\rangle^{\otimes n} = \{|0\rangle_1, \ldots, |0\rangle_n\}$ be an auxiliary system measured by a homodyne measurement M. This measurement serves for the identification of the imperfections of the U_i, $i = 1, \ldots, n$ gates via the $|\varphi_i\rangle$ output systems.

In the system model, each $|0\rangle_i$ auxiliary system is physically realized by a probe beam (e.g., laser or microwave pulse). A particular i-th probe beam is, in fact, a continuous-variable that contains a large number of photons, each of which interacts with the i-th output state, $|\varphi_i\rangle$ (logically, this interaction is represented by the CNOT gate between an i-th pair, $|\varphi_i\rangle$ and $|0\rangle_i$). The n probe beams are then measured by the M homodyne measurement block[39,131], such that n continuous variables are generated on its output.

Without loss of generality, the interaction for an i-th qubit can be described by the effective form of cross-Kerr nonlinearity[39,48–51] via the H_{int}^i interaction Hamiltonian as

$$H_{\mathrm{int}}^i = \hbar\chi_i\sigma_Z a^\dagger a, \tag{4}$$

where χ_i is the strength of the nonlinear interaction, a and $a^\dagger$ are the creation and annihilation operators[39,48–51], and σ_z is the Pauli Z-operator.

Assuming that the interaction holds for a time t_{int}^i for an i-th probe beam $|0\rangle_i$, the interaction causes a rotation in the phase space $\mathscr{S}$ by a particular angle $\pm\theta'_\epsilon$ (i.e., phase shift of $|0\rangle_i$), which is defined as

$$\theta'_\epsilon = \chi_i t_{\mathrm{int}}^i. \tag{5}$$

Then, by $|\varphi_i\rangle$ interacting with the i-th probe beam, the θ'_ϵ angle is as follows:

$$\theta'_\epsilon = \begin{cases} \theta_i, & \text{if } |\varphi_i\rangle = U_i|0\rangle \\ -\theta_i, & \text{if } |\varphi_i\rangle = U_i|1\rangle \\ \theta_i + \Delta_i, & \text{if } |\varphi_i\rangle = V_i|0\rangle \\ -(\theta_i + \lambda_i), & \text{if } |\varphi_i\rangle = Q_i|1\rangle \end{cases}. \tag{6}$$

A detailed description of (6) is as follows: The i-th probe beam picks up a θ_i phase shift if $|\varphi_i\rangle$ is in the state $U_i|0\rangle$ and a $-\theta_i$ phase shift if $|\varphi_i\rangle$ is in the state $U_i|1\rangle$, where U_i is the transformation associated with the i-th unitary gate. Hence, for each U_i, a reference angle θ_i exists that identifies the correct working mechanism of gate U_i. On the other hand, if $|\varphi_i\rangle$ is not in the state $U_i|0\rangle$—i.e., the i-th gate realizes the unitary V_i with output $|\varphi_i\rangle = V_i|0\rangle$, where $V_i \neq U_i$—then the i-th probe beam has a phase shift θ'_ϵ as

$$\theta'_\epsilon = \theta_i + \Delta_i. \tag{7}$$

Specifically, if the i-th gate realizes the unitary Q_i, so $|\varphi_i\rangle$ is not in the state $U_i|1\rangle$, i.e., $|\varphi_i\rangle = Q_i|1\rangle$, where $Q_i \neq U_i$, then the phase shift is as

$$-\theta'_\epsilon = -(\theta_i + \lambda_i). \tag{8}$$

The θ_i reference values are known in the model because the ideal gate unitaries are also known; therefore, the errors Δ_i and λ_i can be determined as follows: Since a coherent state in the phase space is associated with an x position and a p momentum parameter, the M homodyne measurement is in fact a projection of the elements of $\mathscr{S}$ onto the x-axis[39,131]. Therefore, from the $M(|\tilde{0}\rangle_i)$ projection, where $|\tilde{0}\rangle_i$ is the probe beam state after the interaction, the phase shift of the i-th probe beam is evaluated as

$$M(|\tilde{0}\rangle_i) = \begin{cases} x\cos(\theta_i), & \text{if } |\varphi_i\rangle = U_i|0\rangle \\ x\cos(-\theta_i), & \text{if } |\varphi_i\rangle = U_i|1\rangle \\ x\cos(\theta_i + \Delta_i), & \text{if } |\varphi_i\rangle = V_i|0\rangle \\ x\cos(-\theta_i - \lambda_i), & \text{if } |\varphi_i\rangle = Q_i|1\rangle \end{cases}. \tag{9}$$

Thus, from the result $M(|\tilde{0}\rangle_i)$, the quantities Δ_i and λ_i can be determined as

$$\Delta_i = \cos^{-1}\left(\frac{M\left(|\tilde{0}\rangle_i\right)}{x}\right) - \theta_i \tag{10}$$

and

$$\lambda_i = -\left(\cos^{-1}\left(\frac{M\left(|\tilde{0}\rangle_i\right)}{x}\right) + \theta_i\right), \tag{11}$$

where x and θ_i are known parameters. In fact, we do not have to know whether the actual state of $|\varphi_i\rangle$ is $|\varphi_i\rangle = V_i|0\rangle$ or $|\varphi_i\rangle = Q_i|1\rangle$, since only the difference between the actual angle θ'_ϵ and the reference angle θ_i (see (10) and (11)) is required to establish the $\mathscr{C}$ block.

An i-th gate U_i can therefore be referred via the following operations in function of (10) and (11):

$$U_i = \begin{cases} U_i, & \text{if } \Delta_i = 0 \text{ or } \lambda_i = 0 \\ V_i, & \text{if } \Delta_i \neq 0 \\ Q_i, & \text{if } \lambda_i \neq 0 \end{cases}. \tag{12}$$

In the next step, the $|\varphi_i\rangle$ states are entangled by the M_b homodyne measurement block. For a particular pair $\{|\varphi_i\rangle, |\varphi_j\rangle\}$, the aim of the quantum bus[39,48–51] is to achieve the entangled system $|\Phi\rangle = U_i U_j|\beta\rangle$, where $|\beta\rangle$ is a Bell state, while U_i and U_j are the unitaries of the i-th and j-th unitary gates. After the M_b measurement, the operations U_i and U_j therefore formulate the entangled system $U_i U_j$, since $|\varphi_i\rangle = U_i|\psi_i\rangle$ and $|\varphi_j\rangle = U_j|\psi_j\rangle$ for some inputs $|\psi_i\rangle$ and $|\psi_j\rangle$.

The interaction Hamiltonian for the probe beam $|0\rangle_b$ is $H_{\mathrm{int}} = \hbar\chi_b\sigma_z a^\dagger a$, where χ_b is the strength of the nonlinear interaction[39,48–51]. For a given interaction time t_b, the interaction with a particular $|\varphi_i\rangle$ causes a rotation $\pm\omega_i^b$
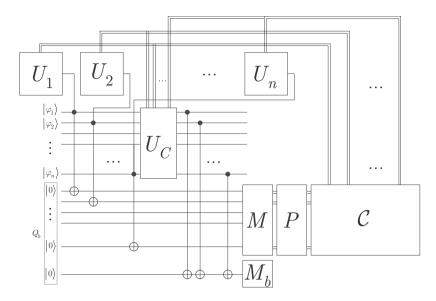
Figure 1. Schematic model of the unsupervised quantum gate control mechanism. The output states $|\varphi_1\rangle \dots |\varphi_n\rangle$ of unitaries U_i, $i = 1, \dots, n$ of the quantum computer are placed onto the qubus Q_b (depicted by dashed frame). For each U_i, a reference phase state angle θ_i is defined. For each $|\varphi_i\rangle$ an auxiliary system $|0\rangle_i$ is set using CNOT gates. The auxiliary qubits are measured by the first homodyne measurement block M. The measurement results (double lines refer to classical information) are processed by a P post-processing block, and by a $\mathscr{C}$ machine learning control block. Using the results of $\mathscr{C}$, operator U_C corrects of the $|\varphi_i\rangle$ states on Q_b. The second homodyne measurement, M_b, entangles the corrected states of Q_b using the probe beam $|0\rangle_b$.

in the angle of the probe beam $|0\rangle_b$ with angle $\omega_i^b = \chi_b t_b$. For a corrected pair $\{|\varphi_i\rangle, |\varphi_j\rangle\}$, the result of the $M_b(|0\rangle_b)$ homodyne measurement is $x \cos(\omega_i^b + \omega_j^b)$ or $x \cos(\omega_i^b - \omega_j^b)$. This is because for $\{|\varphi_i\rangle, |\varphi_j\rangle\} = U_i|0\rangle_i U_j|0\rangle_j$ or $\{|\varphi_i\rangle, |\varphi_j\rangle\} = U_i|1\rangle_i U_j|1\rangle_j$, the probe beam $|0\rangle_b$ is shifted by ω_i^b for a $U_i|0\rangle$ state and by $-\omega_i^b$ for a $U_i|1\rangle$ state; thus, in this case, the phase shift is $\omega_i^b + \omega_j^b$. On the other hand, if $\{|\varphi_i\rangle, |\varphi_j\rangle\} = U_i|0\rangle_i U_j|1\rangle_j$ or $\{|\varphi_i\rangle, |\varphi_j\rangle\} = U_i|1\rangle_i U_j|0\rangle_j$, the resulting phase shift is $|\omega_i^b - \omega_j^b|$, which yields $x \cos(\omega_i^b - \omega_j^b)$. If $M_b(|0\rangle_b)$ results in $x \cos(\omega_i^b - \omega_j^b)$, an auxiliary NOT gate is applied to either qubit of an ij pair $\{|\varphi_i\rangle, |\varphi_j\rangle\}$.

Therefore, the unstable and stable quantum gates can be identified via Q_b and M, that concludes the proof. ∎

NISQ applications.   A straightforward NISQ[1] application of the system model is in trapped ion scenarios or in superconducting circuits. The explicit number of gates, gate fidelities, and total error of the protocol are external parameters in the system model that depend on the actual physical-layer apparatus. The control theory behind the system model and the definition of the machine learning control unit makes implementable the results via near-term technologies in experiment. In particular, a near-term application is in qubit gate-model quantum computer architectures considering the case of a large number of qubits and quantum gates, $n \gg 1$[2,5–7]. As a future work, our aim is to analyze the performance of the system model in these scenarios.

The proposed system model utilizes a Q_b quantum bus, however U_C controlling block, the P post-processing block and the $\mathscr{C}$ machine learning control block can also be implemented in different practical scenarios. As follows, the system model is not limited for quantum buses allowing a widespread application in experiment. Other practical application scenarios of the results include measurement control problems and measurement optimization in quantum computations, qubit control and readout, objective function evaluation in gate-model quantum computes for solving optimization problems, and optimization of tasks of measurement-based quantum information processing. An aim is to extend the application of the proposed system model into these directions also.

The schematic model of the quantum gate controlling method is depicted in Fig. 1[47]. For simplicity, the figure shows only one-qubit unitaries, however the results hold for arbitrary quantum gates. The U_C, P, and $\mathscr{C}$ operations are defined in Section 4.

Quantum gate control

The aim of the $\mathscr{C}$ block is to achieve a machine learning–based method for controlling the unitary gates using the results of the M homodyne measurement block post-processed by P. The U_C operation for controlling the quantum states directly on the qubus is also defined. First, we give the problem statement in terms of control theory[115–117].

Method.   Let us assume that for each i-th quantum system $|\varphi_i\rangle$, a reference angle θ_i is defined (see Theorem 1). This angle identifies a correct working mechanism of the unitary gate U_i. Focusing on qubit gates, for an i-th gate, the reference operation U_i is defined as

$$U_i = \exp(-iH_i t_{U_i}/\hbar) = \cos(t_{U_i}/\hbar)I - i \sin(t_{U_i}/\hbar)H_{U_i}, \tag{13}$$

where t_{U_i} is the application time of unitary U_i, $\hbar$ is the reduced Planck constant (we set $\hbar = 1$), and I is the identity operator, while H_{U_i} is a Hamiltonian with energy E_i:

$$E_i = \frac{1}{2}\hbar 2\pi(f_i), \tag{14}$$

where f_i is the frequency:

$$f_i = \frac{1}{T_i} \tag{15}$$

where T_i is the period time.

Focusing on a particular pair $\{|\varphi_i\rangle, |\varphi_j\rangle\}$, the corresponding U_i and U_j reference operations are identified as follows: Let us assume that the application time of the U_i unitary is t_{U_i}, with period time $\pi_i = T_i = z t_{U_i}$, $z > 0$, and for U_j, the application time is t_{U_j}, with period time $\pi_j = T_j = y t_{U_j}$, $y > 0$. Then, by introducing quantities A and B for U_i, as

$$A = \cos(t_{U_i}), \tag{16}$$

$$B = \sin(t_{U_i}), \tag{17}$$

and quantities C and D for U_j, as

$$C = \cos(t_{U_j}), \tag{18}$$

$$D = \sin(t_{U_j}), \tag{19}$$

the U_i and U_j operations can be rewritten as

$$U_i = AI - iBH_{U_i}, \tag{20}$$

and

$$U_j = CI - iDH_{U_j}, \tag{21}$$

with the corresponding Hamiltonians H_{U_i}, H_{U_j}. The related energy operators are $E_i = \frac{1}{2}\hbar 2\pi(f_i)$, $E_j = \frac{1}{2}\hbar 2\pi(f_j)$, where $f_i = \frac{1}{T_i}$ and $f_j = \frac{1}{T_j}$.

In the control problem, we assume a scenario in which the U_i gate works improperly, which leads to imperfect oscillations, while U_j works perfectly. The aim of the $\mathscr{C}$ is to achieve the stabilization of U_i using the fact that M_b creates the entangled structure $U_i U_j$, since M_b entangles the qubus states. The challenge here is therefore the stabilization of U_i such that it randomly oscillates (i.e., U_i is non-stable) while U_j is stable in $U_i U_j$. In the control problem, this random oscillation cannot be corrected by a controlling parameter applied directly to U_i. The problem is then to find a way to correct the random oscillations by exploiting the fact that $U_i U_j$ is an entangled structure.

As we show in Theorem 2, in an entangled structure $U_i U_j$, it is possible to fix the random oscillations of U_i by controlling U_j. On the other hand, if $U_i \otimes U_j$ is a product system, then calibration is not possible.

Theorem 2 (Controlling of entangled gate structure). *In an entangled gate structure $U_i U_j$, a randomly oscillating non-stable gate U_i is controllable via a stable gate U_j. In a product system $U_i \otimes U_j$, the non-stable gate U_i is not controllable via the control of a stable gate U_j.*

Proof. First, let assume that U_i and U_j are formulating the entangled structure $U_i U_j$ via the M_b measurement on the qubus. Using the parameters A, B of U_i (see (16) and (17)) and C, D of U_j (see (18) and (19)), the controlling problem in terms of control theory[115–117] is as follows.

Using a Galerkin expansion and a generalized mean-field system formulation[115] for the description of the controlling, for a non-stable gate U_i in the joint system $U_i U_j$, a growth rate[115–117] parameter μ_i is defined as

$$\mu_i = \beta_i^0 - \beta_i^i(A^2 + B^2) - \beta_i^j(C^2 + D^2), \tag{22}$$

where β_i^0 is the initial growth rate[115–117], β_i^i is the parameter for growth-rate change of μ_i due to $\sqrt{(A^2 + B^2)}$, while β_i^j is the parameter for growth-rate of μ_i due to $\sqrt{(C^2 + D^2)}$ for U_i.

Then, let $D_t(x) = dx/dt$, and define sets $\mathscr{C}_{U_i}$: $\{D_t(A), D_t(B)\}$ and $\mathscr{C}_{U_j}$: $\{D_t(C), D_t(D)\}$. For U_i, the quantity $D_t(A)$ in set $\mathscr{C}_{U_i}$ is as

$$D_t(A) = \mu_i A - F_i B, \tag{23}$$

where F_i is a parameter for the frequency defined as

$$F_i = f_i + \delta_i^i(A^2 + B^2) + \delta_i^j(C^2 + D^2), \tag{24}$$

where f_i is the initial frequency, $f_i = \frac{1}{T_i}$, δ_i^i is a parameter for frequency-change due to term $\sqrt{(A^2 + B^2)}$, while δ_i^j is a parameter for frequency-change due to term $\sqrt{(C^2 + D^2)}$; while $D_t(B)$ in $\mathscr{C}_{U_i}$ is as

$$D_t(B) = F_i A + \mu_i B. \tag{25}$$

For unitary U_j, we define μ_j as

$$\mu_j = \beta_j^0 - \beta_j^i(A^2 + B^2) - \beta_j^j(C^2 + D^2), \tag{26}$$

where β_j^0 is the initial growth rate, β_j^i the parameter for growth-rate of μ_j due to $\sqrt{(A^2 + B^2)}$, while β_j^j is the parameter for growth-rate of μ_j due to $\sqrt{(C^2 + D^2)}$; and $D_t(C)$ from $\mathscr{C}_{U_j}$ is as

$$D_t(C) = \mu_j C - F_j D, \tag{27}$$

where F_j is a parameter for the frequency as

$$F_j = f_j + \delta_j^i(A^2 + B^2) + \delta_j^j(C^2 + D^2), \tag{28}$$

where f_j is the initial frequency, $f_j = \frac{1}{T_j}$, δ_j^i is a parameter for frequency-change due to $\sqrt{(A^2 + B^2)}$, while δ_j^j is a parameter for frequency-change due to $\sqrt{(C^2 + D^2)}$; and $D_t(D)$ from $\mathscr{C}_{U_j}$ is as

$$D_t(D) = F_j C + \mu_j D + \partial, \tag{29}$$

where ∂ is a control parameter.

Since for the $U_i U_j$ entangled structure, in (22) the terms $\beta_i^i(A^2 + B^2)$ and $\beta_i^j(C^2 + D^2)$ are non-vanishing, making the U_i gate to be controllable via U_j. This connection still holds for $U_i U_j$ after some simplifications of the system model.

Let simplify the description $U_i U_j$, as follows. For U_i, let use $F_i = 1$, and set $\beta_i^i = \beta_i^j = 1$ in (22). Then, by using (20) and (21), we redefine (22) as

$$\mu_i = \beta_i^0 - (A^2 + B^2) - (C^2 + D^2). \tag{30}$$

After the M_b measurement, the yielding system of U_i can be evaluated via (30) as

$$D_t(A) = \mu_i A - B, \tag{31}$$

and

$$D_t(B) = A + \mu_i B. \tag{32}$$

For U_j, set $\beta_j^i = \beta_j^j = 0$, thus (26) can be rewritten as

$$\mu_j = \beta_j^0, \tag{33}$$

and set $\delta_j^i = \delta_j^j = 0$ in (28), thus (28) can be rewritten as

$$F_j = f_j = \frac{1}{T_j}. \tag{34}$$

Thus, (27) and (29) can be reevaluated as

$$D_t(C) = \beta_j^0 C - f_j D, \tag{35}$$

and

$$D_t(D) = \beta_j^0 D + f_j C + \partial. \tag{36}$$

As follows, for the simplified model (30–36) of $U_i U_j$, the U_i gate remains controllable via U_j since terms $\beta_i^i(A^2 + B^2)$ and $\beta_i^j(C^2 + D^2)$ are non-vanishing in (30). However, this is not the case if $U_i \otimes U_j$ formulate a product state system with unentangled gates.

The system model of the product system $U_i \otimes U_j$ is derived follows. Let assume that gates U_i and U_j are formulating a product state system $U_i \otimes U_j$. In this case, the gates U_i and U_j in $U_i \otimes U_j$ are unentangled, thus modifications required in the system model.

In terms of control theory, the $U_i \otimes U_j$ product system is analogous to a linearization around the $A^2 = B^2 = C^2 = D^2 = 0$ (fixed point of the model). This linearization breaks the entangled structure $U_i U_j$, leading to $\beta_i^i = \beta_i^j = \beta_j^i = \beta_j^j = 0$, and $\delta_i^i = \delta_i^j = \delta_j^i = \delta_j^j = 0$.

Thus, for $U_i \otimes U_j$, the terms $\beta_i^i(A^2 + B^2)$ and $\beta_i^j(C^2 + D^2)$ are vanishing in (22), thus (22) picks up the formula of

$$\mu_i = \beta_i^0, \tag{37}$$

thus the resulting system model for $U_i \otimes U_j$ is as

$$D_t(A) = \beta_i^0 A - f_i B, \tag{38}$$

$$D_t(B) = f_i A + \beta_i^0 B. \tag{39}$$

$$D_t(C) = \beta_j^0 C - f_j D, \tag{40}$$

and

$$D_t(D) = f_j C + \beta_j^0 D + \partial. \tag{41}$$

As follows from the system model (38–41) of $U_i \otimes U_j$, for U_i the quantity $\sqrt{A^2 + B^2}$ grows without bound (i.e., U_i is non-stable), while for U_j, the quantity $\sqrt{C^2 + D^2}$ converges to zero for $\partial = 0$ (i.e., U_j is stable)[115–117]. Thus, in terms of control theory, in system (38–41), the randomly fluctuating quantum gate U_i cannot controlled by U_j. As a corollary, while U_i is controllable in the entangled structure $U_i U_j$, in a tensor product system $U_i \otimes U_j$ is not controllable.

The proof is concluded here. ∎

Cost function. The cost function $f_C(U_i U_j)$ for the controlling of the $U_i U_j$ entangled gate structure is a subject to a minimization, and defined as

$$f_C(U_i U_j) = \widetilde{f}_{U_i} + \gamma f_\partial \tag{42}$$

where

$$\widetilde{f}_{U_i} = A^2 + B^2 \tag{43}$$

and

$$f_\partial = \partial^2, \tag{44}$$

where ∂ is the control parameter (75), while γ is a penalization parameter[115–117].

Let $C(U_i U_j)$ be a control function defined for the joint structure $U_i U_j$ as

$$\partial = C(U_i U_j), \tag{45}$$

and let $\Pr(A, B, C, D)$ be the probability density associated to a current values of A, B, C, D of the entangled structure $U_i U_j$. At a particular A, B of U_i, the result of ∂ on U_i can be evaluated by the $\partial_{U_i} = \mathbb{E}(C(U_i U_j)|A, B)$ expectation value as

$$\partial_{U_i} = \int\int \Pr(A, B, C, D) C(U_i U_j) dC dD. \tag{46}$$

At a given C, D of U_j, the result of ∂ on U_j can be evaluated the expectation value $\partial_{U_j} = \mathbb{E}(C(U_i U_j)|C, D)$ as

$$\partial_{U_j} = \iint \Pr(A, B, C, D) C(U_i U_j) dA dB. \tag{47}$$

The terms (45), (46) and (47) will be specified further in Section 5 via the determination of the controlling function $C(U_i U_j)$.

Post-processing. **Lemma 1** *P post-processing on the results of the M homodyne measurement yields the estimations of the unitaries of the quantum gates.*

Proof. Focusing on a gate-pair $\{U_i, U_j\}$, the aim of the P post-processing method is to achieve the estimates $\widetilde{A}, \widetilde{B}$ and $\widetilde{C}, \widetilde{D}$ using the results of the M measurement. The estimated quantities are then fed into the $\mathscr{C}$ block that achieves the automated control of the quantum gates.

The quantities A, B C, and D are derived from the M measurement as follows: Let us focus on a i-th unitary U_i with quantities A, B and reference phase space angle θ_i. The quantities Δ_i (10) and λ_i (11) are also computed in the P post-processing phase using the $M(|\bar{0}\rangle_i)$ measurement (see (9)) of the i-th probe beam $|\bar{0}\rangle_i$. These steps yield the estimates $\widetilde{A}$ and $\widetilde{B}$ as follows. At a particular t_{U_i} application time of U_i, at $\Delta_i = 0$ or $\lambda_i = 0$,

$$\widetilde{A} = \cos(\varsigma_i \theta_i) = \cos(t_{U_i}), \tag{48}$$

$$\widetilde{B} = \sin(\varsigma_i \theta_i) = \sin(t_{U_i}), \tag{49}$$

where

$$\varsigma_i = \frac{t_{U_i}}{\theta_i}. \tag{50}$$

Therefore, for $\Delta_i \neq 0$, the V_i unitary is performed instead of U_i:

$$\widetilde{A} = \cos(\varsigma_i(\theta_i + \phi_i)) = \cos(t_{U_i} + t_{\phi_i}), \tag{51}$$

$$\widetilde{B} = \sin(\varsigma_i(\theta_i + \phi_i)) = \sin(t_{U_i} + t_{\phi_i}), \tag{52}$$

where

$$\phi_i = \begin{cases} \Delta_i, & \text{if } \theta'_\epsilon < \theta_i \\ -\Delta_i, & \text{if } \theta'_\epsilon > \theta_i \end{cases}, \tag{53}$$

where θ'_ϵ is given in (7), and t_{ϕ_i} is as

$$t_{\phi_i} = \varsigma_i(\theta_i + \phi_i) - t_{U_i}. \tag{54}$$

For $\lambda_i \neq 0$, the Q_i unitary is performed instead of U_i; thus,

$$\widetilde{A} = \cos(\varsigma_i(\theta_i + \varphi_i)) = \cos(t_{U_i} + t_{\varphi_i}), \tag{55}$$

$$\widetilde{B} = \sin(\varsigma_i(\theta_i + \varphi_i)) = \sin(t_{U_i} + t_{\varphi_i}), \tag{56}$$

where

$$\varphi_i = \begin{cases} -\lambda_i, & \text{if } -\theta'_\epsilon > -\theta_i \\ \lambda_i, & \text{if } -\theta'_\epsilon < -\theta_i \end{cases}, \tag{57}$$

where $-\theta'_i$ is as given in (8) and t_{φ_i} is as

$$t_{\varphi_i} = \varsigma_i(\theta_i + \varphi_i) - t_{U_i}. \tag{58}$$

These results straightforwardly follow for U_j, with the corresponding parameters $\Delta_j, \lambda_j, t_{U_j}$, reference angle θ_j, and ς_j. ∎

The machine learning–based control of the randomly oscillating non-stable gate U_i in the $U_i U_j$ joint structure is discussed in Section 5.

Unsupervised Control of Entangled Gates

Theorem 3 (*Quantum gate calibration*). *For an entangled gate structure U_iU_j with a non-stable U_i, the $\mathscr{C}$ block calibrates the quantum gates via the optimal control function $C^*(U_iU_j) = \sqrt{\overline{L}_{act}}$, where $\overline{L}_{act} = \prod^2\beta_i^0/0.2((\widetilde{A}^2 + \widetilde{B}^2) + (\widetilde{C}^2 + \widetilde{D}^2))$, where $\prod$ is a controlling amplitude, while $\widetilde{A}, \widetilde{B}, \widetilde{C}, \widetilde{D}$ are determined via P post-processing.*

Proof. The $\mathscr{C}$ block gets as input the post-processed results $P(M(|\widetilde{0}\rangle_i))$, $i = 1, \ldots, n$. The $C(\widetilde{A}, \widetilde{B}, \widetilde{C}, \widetilde{D})$ control function of the joint system U_iU_j is evaluated via the $\mathscr{C}$ block, where $\widetilde{A}, \widetilde{B}, \widetilde{C}, \widetilde{D}$ are determined by P post-processing step.

The $\mathscr{C}$ block operates via a set $\mathscr{S}_f$ of operations, as

$$\mathscr{S}_f: \{S_e, S_t\}, \tag{59}$$

where s_e is a set of elementary operations $S_e = \{\pm, \times, /\}$, while $S_t = \{\exp, \sin, \ln, \tanh\}$ is a set of transcendental functions[115–117].

Focusing on a particular pair of unitaries $\{U_iU_j\}$, where U_i is not stable while U_j is a stable gate, the $\mathscr{C}$ block iterates until the optimal control function $C^*(U_iU_j)$ is determined. The output of the $\mathscr{C}$ block is the ∂^* optimal control parameter of the for the joint structure U_iU_j, as

$$\begin{aligned} \partial^* &= \iint \Pr(\widetilde{A}, \widetilde{B}, \widetilde{C}, \widetilde{D})C^*(\widetilde{A}, \widetilde{B}, \widetilde{C}, \widetilde{D})d\widetilde{A}\,d\widetilde{B}\,d\widetilde{C}\,d\widetilde{D} \\ &= \partial_1\partial_2, \end{aligned} \tag{60}$$

where $\Pr(\widetilde{A}, \widetilde{B}, \widetilde{C}, \widetilde{D})$ is the probability density associated with $\widetilde{A}, \widetilde{B}, \widetilde{C}, \widetilde{D}$, while ∂_1 is a control parameter for the joint structure U_iU_j as

$$\partial_1 = C^*(\widetilde{A}, \widetilde{B}, \widetilde{C}, \widetilde{D}), \tag{61}$$

where $C^*(\widetilde{A}, \widetilde{B}, \widetilde{C}, \widetilde{D})$ is an optimal control function using the post-processing results $\widetilde{A}, \widetilde{B}, \widetilde{C}, \widetilde{D}$, while ∂_2 is a stabilization parameter associated with the stable gate U_j, as

$$\partial_2 = \iint \Pr(\widetilde{A}, \widetilde{B}, \widetilde{C}, \widetilde{D})C^*(\widetilde{A}, \widetilde{B}, \widetilde{C}, \widetilde{D})d\widetilde{A}\,d\widetilde{B} = C^*(\widetilde{D}). \tag{62}$$

From (60), (61), and (62), $C^*(U_iU_j)$ is yielded as

$$C^*(U_iU_j) = \partial^* = C^*(\widetilde{A}, \widetilde{B}, \widetilde{C}, \widetilde{D})C^*(\widetilde{D}), \tag{63}$$

such that the quantities of (61) and (62) are determined by $\mathscr{C}$ using the set of (59).

We also give the form of $C^*(U_iU_j)$ with respect to the cost function $f_C(U_iU_j)$. For this purpose, we also introduce time parameters for the controlling mechanism.

Let T_L be the time interval defined for the controlling as

$$T_L = \ln\left(\frac{\sqrt{\overline{A}^2 + \overline{B}^2}}{\sqrt{\underline{A}^2 + \underline{B}^2}}\right)\frac{1}{-\vartheta}, \tag{64}$$

where $\overline{x}, \underline{x}$ refer to the upper and lower bound on x, while ϑ is a decay rate parameter for the controlling, defined as

$$\vartheta = \beta_i^0 - (\widetilde{A}^2 + \widetilde{B}^2) - (\widetilde{C}^2 + \widetilde{D}^2). \tag{65}$$

For the activation of the $\mathscr{C}$ block, the A_L activation parameter is defined as

$$\begin{aligned} A_L &= h\left(\left(\sqrt{\widetilde{A}^2 + \widetilde{B}^2}\right) - \left(\sqrt{\overline{A}^2 + \overline{B}^2}\right)\right) \\ &\quad -h\left((\sqrt{\underline{A}^2 + \underline{B}^2}) - \left(\sqrt{\widetilde{A}^2 + \widetilde{B}^2}\right)\right) \\ &\quad +h\left(\left(\sqrt{\widetilde{C}^2 + \widetilde{D}^2}\right) - \beta_i^0\right), \end{aligned} \tag{66}$$

where $h(\cdot)$ is the Heaviside function[115–117] and β_i^0 is as shown in (22). As $A_L > 0$, the $\mathscr{C}$ block starts the calibration of the quantum gates; otherwise, there is no calibration in the system.

Then let T_P be the period time for one controlling cycle, defined as

$$T_P = T_L + T_{\overline{L}}, \tag{67}$$

where $T_{\overline{L}}$ refers to an uncontrolled period, defined via β_i^0 as

$$T_{\overline{L}} = \ln\left(\frac{\sqrt{\overline{A}^2 + \overline{B}^2}}{\sqrt{\underline{A}^2 + \underline{B}^2}}\right)\frac{1}{\beta_i^0}. \tag{68}$$

Let $\prod$ be the controlling amplitude and L_{act}^{max} be maximal actuation level, as

$$L_{act}^{max} = \frac{\Pi^2}{2}. \tag{69}$$

Using $\prod$ and a quasi-equilibrium assumption[115–117], the parameter of (65) can be rewritten as

$$\vartheta = \beta_i^0 - \ell\Pi^2 = \beta_i^0 - \ell 2 L_{act}^{max}, \tag{70}$$

where l is defined as

$$\ell = \frac{(\widetilde{A}^2 + \widetilde{B}^2) + (\widetilde{C}^2 + \widetilde{D}^2)}{\Pi^2}. \tag{71}$$

The f_{∂^*} cost in function $f_C(U_iU_j)$ is therefore analogous to an $\overline{L}_{act}$ average actuation level at a particular $\widetilde{A}$ and $\widetilde{B}$, as

$$f_C(U_iU_j) = (\widetilde{A}^2 + \widetilde{B}^2) + \gamma\overline{L}_{act}, \tag{72}$$

where γ is as in (42), while $\overline{L}_{act}$ is as

$$\begin{aligned}
\overline{L}_{act} &= \left(\frac{T_L}{T_P}\right)L_{act}^{max} = \left(\frac{\beta_i^0}{\ell\Pi^2}\right)\frac{\Pi^2}{2} \\
&= \frac{\beta_i^0}{2\ell} = \frac{\Pi^2\beta_i^0}{2((\widetilde{A}^2 + \widetilde{B}^2) + (\widetilde{C}^2 + \widetilde{D}^2))}.
\end{aligned} \tag{73}$$

The optimal $\partial^* = C^*(U_iU_j)$ control function is therefore as

$$\begin{aligned}
C^*(U_iU_j) &= \underset{\forall C(U_iU_j)}{\operatorname{argmin}} f_C(U_iU_j) \\
&= \sqrt{\overline{L}_{act}} \\
&= \sqrt{\frac{\Pi^2\beta_i^0}{2((\widetilde{A}^2 + \widetilde{B}^2) + (\widetilde{C}^2 + \widetilde{D}^2))}} \\
&= \partial^*,
\end{aligned} \tag{74}$$

where $f_C(U_iU_j)$ is the cost function defined in (72).

The proof is concluded here. ∎

Direct L algorithm. Here we give the steps of the $\mathscr{C}$ controlling procedure assuming that there is no activation function (66) in the $\mathscr{C}$ block (referred to as Direct L Algorithm) and the U_iU_j system is simplified as given by (31–36). The steps are summarized in Algorithm A.1.

Algorithm 1 Direct L Algorithm

Input: Set a $U_i U_j$ structure with a non-stable U_i and a stable U_j gate, as characterized by (31)–(36).

Output: Optimal control function $C^*(U_i U_j)$ that minimizes (42).

Step 1. Parameterize the $\mathscr{C}$ block via set (59).

Step 2. Set the ∂ control parameter of cost function (44) as

$$\partial = C(U_i U_j) = C(A, B, C, D), \tag{75}$$

where $C(\cdot)$ is a control function.

Step 3. Set γ and determine the optimal $C^*(U_i U_j)$ control function, as

$$C^*(U_i U_j) = \underset{\forall C(U_i U_j)}{\arg\min} f_C(U_i U_j), \tag{76}$$

where $f_C(U_i U_j)$ is the cost function defined in (42).

Step 4. Set the n_G number of generations parameter and n_I number of iterations parameter.

Step 5. For all k, $k = 1, \dots, n_G$, compute the cost function (42) as $f_C^{k,l}(U_i U_j) = \tilde{f}_{U_i}^{k,l} + \gamma f_{\partial}^{k,l}$, where $\mathscr{C}$, $l = 1, \dots, n_I$, with $\tilde{f}_{U_i}^{k,l} = A_{k,l}^2 + B_{k,l}^2$, $f_{\partial}^{k,l} = C_{k,l}(U_i U_j)$, where parameters $A_{k,l}^2$, $B_{k,l}^2$, and $C_{k,l}(U_i U_j)$ are associated with $\{k, l\}$ indices.

Step 6. Select the minimal $f_C^*(U_i U_j) = \underset{\forall k,l}{\arg\min} f_C^{k,l}(U_i U_j)$ cost function from the $N_{tot} = n_G n_I$ total number of solutions.

Step 7. Output the optimal control function $C^*(U_i U_j)$ associated with f_{∂}^* in $f_C^*(U_i U_j)$.

Controlling on the quantum bus.   **Lemma 2** *The quantum states placed onto the qubus can be calibrated by operation U_C.*

Proof. The proof assumes that the aim of U_C is the correction of the qubus states before the M_b measurement is performed.

The $|\varphi_i\rangle$, $i = 1, \dots, n$ quantum states placed onto the qubus are transformed into the reference state by the $U_C = \{U_C^1, \dots, U_C^n\}$ operation (qubus operation), where U_C^i is the operation associated with the i-th qubit. The controlling is as follows.

Since for a particular $|\varphi_i\rangle$, the difference in the reference phase space angle $\pm\theta_i$ of an i-th gate U_i can be identified by (10) and (11) via the M measurement and P post-processing, for $\Delta_i \neq 0$, a correction operator U_C^{i,Δ_i} can be straightforwardly defined as

$$U_C^{i,\Delta_i} = e^{i\varsigma} R_C^{i,\Delta_i}(\eta_i), \tag{77}$$

where ς is a real number, and $R_C^{i,\Delta_i}(\eta_i)$ is as

$$R_C^{i,\Delta_i}(\eta_i) = \cos\left(\frac{\eta_i}{2}\right) I - i \sin\left(\frac{\eta_i}{2}\right) \bar{n} \cdot \overrightarrow{\sigma} = \exp\left(-i\frac{\eta_i}{2}\bar{n} \cdot \overrightarrow{\sigma}\right), \tag{78}$$

where $\bar{n}$ is a unit vector as $\bar{n} = (n_x, n_y, n_z) = (a/L, b/L, c/L)$, where a, b, c and $\mathscr{C}$ are real numbers determined by the H_C^{i,Δ_i} correction Hamiltonian H_C^{i,Δ_i}, as

$$H_C^{i,\Delta_i} = a\sigma_X + b\sigma_Y + c\sigma_Z = L\bar{n} \cdot \overrightarrow{\sigma}, \tag{79}$$

where $L = \sqrt{a^2 + b^2 + c^2}$, while $\overrightarrow{\sigma} = (\sigma_X, \sigma_Y, \sigma_Z)$ is the Pauli vector, $(\bar{n} \cdot \overrightarrow{\sigma})^2 = I$, and

$$\eta_i = \begin{cases} |\varsigma_i \phi_i|, & \text{if } \theta_\epsilon' < \theta_i \\ 2\pi - |\varsigma_i \phi_i|, & \text{if } \theta_\epsilon' > \theta_i \end{cases}, \tag{80}$$

where ϕ_i is given in (53).

For $\lambda_i \neq 0$, a correction operator U_C^{i,λ_i} can be straightforwardly defined as

$$U_C^{i,\lambda_i} = e^{i\varsigma} R_C^{i,\lambda_i}(\nu_i), \tag{81}$$

where

$$R_C^{i,\lambda_i}(\nu_i) = \cos\frac{\nu_i}{2} I - i \sin\frac{\nu_i}{2}\bar{n} \cdot \overrightarrow{\sigma} = \exp\left(-i\frac{\nu_i}{2}\bar{n} \cdot \overrightarrow{\sigma}\right), \tag{82}$$

where

$$\nu_i = \begin{cases} 2\pi - |\varsigma_i \varphi_i|, & \text{if } -\theta'_i > -\theta_i, \\ |\varsigma_i \varphi_i|, & \text{if } -\theta'_i < -\theta_i \end{cases},$$

(83)

where φ_i is given in (57), and with the corresponding a, b, c and $\mathscr{C}$ parameters of the Hamiltonian H_C^{i,λ_i}. The operators (77) and (82) therefore calibrate the qubit onto the reference position $|\varphi_i\rangle = U_i|0\rangle$ or $|\varphi_i\rangle = U_i|1\rangle$ associated with the reference angle $\pm\theta_i$ via Δ_i (10) and λ_i (11), yielded by the M measurement. If $\Delta_i = 0$ or $\lambda_i = 0$, then $|\varphi_i\rangle$ is in the correct position; therefore, $U_C^i = I$; thus, the final form of U_C^i is

$$U_C^i = \begin{cases} U_C^{i,\Delta_i}, & \text{if } \Delta_i \neq 0 \\ U_C^{i,\lambda_i}, & \text{if } \lambda_i \neq 0 \\ I, & \text{if } \Delta_i = 0 \text{ or } \lambda_i = 0 \end{cases}.$$

(84)

The proof is therefore concluded here. ∎

Conclusions

Here, we defined a method for unsupervised control of entangled quantum gates in gate-model quantum computers and near-term quantum devices. The framework utilizes the terms of control theory for the description of the control problem. The system model uses the quantum bus scheme that correlates the gate outputs with auxiliary probe beams. The probe states are measured to provide information to a post-processing unit and are then inputted into the machine learning control. The entangled gate structure is achieved by a second measurement block that entangles the gate outputs, leading to an entangled gate structure. We showed that if the quantum gates are entangled, the non-stable gate is controllable by a stable quantum gate; however, if the gates formulate a product system, then the random oscillations of the non-stable gate are not controllable in terms of control theory. The solution stabilizes the quantum gate structure via the derivation of an optimal control function that minimizes a particular cost function. The framework provides an implementable solution for experimental quantum computations and for near-term quantum computer architectures in the quantum Internet.

Submission note. Parts of this work were presented in conference proceedings[47].

Ethics statement. This work did not involve any active collection of human data.

References

1. Preskill, J. Quantum Computing in the NISQ era and beyond. *Quantum* **2**, 79 (2018).
2. Arute, F. *et al*. Quantum supremacy using a programmable superconducting processor, *Nature*, Vol 574, https://doi.org/10.1038/s41586-019-1666-5 (2019).
3. Aaronson, S. & Chen, L. Complexity-theoretic foundations of quantum supremacy experiments. *Proceedings of the 32nd Computational Complexity Conference*, CCC '17, pages 22:1–22:67 (2017).
4. Harrow, A. W. & Montanaro, A. Quantum Computational Supremacy. *Nature* **549**, 203–209 (2017).
5. Foxen, B. *et al*. Demonstrating a Continuous Set of Two-qubit Gates for Near-term Quantum Algorithms, *arXiv:2001.08343* (2020).
6. Harrigan, M. *et al*. Quantum Approximate Optimization of Non-Planar Graph Problems on a Planar Superconducting Processor, *arXiv:2004.04197v1* (2020).
7. Rubin, N. *et al*. Hartree-Fock on a superconducting qubit quantum computer, *arXiv:2004.04174v1* (2020).
8. Alexeev, Y. *et al*. Quantum Computer Systems for Scientific Discovery, *arXiv:1912.07577* (2019).
9. Loncar, M. *et al*. Development of Quantum InterConnects for Next-Generation Information Technologies, *arXiv:1912.06642* (2019).
10. Ajagekar, A., Humble, T. & You, F. Quantum Computing based Hybrid Solution Strategies for Large-scale Discrete-Continuous Optimization Problems. *Computers and Chemical Engineering* Vol 132, 106630 (2020).
11. Ajagekar, A. & You, F. Quantum computing for energy systems optimization: Challenges and opportunities. *Energy* **ume 179**, 76–89 (2019).
12. Lloyd, S. Quantum approximate optimization is computationally universal, *arXiv:1812.11075* (2018).
13. Farhi, E., Goldstone, J. & Gutmann, S. A Quantum Approximate Optimization Algorithm. *arXiv:1411.4028*. (2014).
14. Farhi, E., Goldstone, J., Gutmann, S. & Neven, H. Quantum Algorithms for Fixed Qubit Architectures. *arXiv:1703.06199v1* (2017).
15. Farhi, E. & Neven, H. Classification with Quantum Neural Networks on Near Term Processors, *arXiv:1802.06002v1* (2018).
16. Farhi, E., Goldstone, J., Gutmann, S. & Zhou, L. The Quantum Approximate Optimization Algorithm and the Sherrington-Kirkpatrick Model at Infinite Size, *arXiv:1910.08187* (2019).
17. Farhi, E., Gamarnik, D. & Gutmann, S. The Quantum Approximate Optimization Algorithm Needs to See the Whole Graph: Worst Case Examples, *arXiv:2005.08747* (2020).
18. Farhi, E., Goldstone, J. & Gutmann, S. A Quantum Approximate Optimization Algorithm Applied to a Bounded Occurrence Constraint Problem. *arXiv:1412.6062*. (2014).
19. IBM. *A new way of thinking: The IBM quantum experience*, http://www.research.ibm.com/quantum (2017).
20. Van Meter, R. *Quantum Networking*, John Wiley and Sons Ltd, ISBN 1118648927, 9781118648926 (2014).
21. Gyongyosi, L. Quantum State Optimization and Computational Pathway Evaluation for Gate-Model Quantum Computers, *Scientific Reports*, https://doi.org/10.1038/s41598-020-61316-4 (2020).
22. Shor, P. W. Algorithms for quantum computation: discrete logarithms and factoring. In: *Proceedings of the 35th Annual Symposium on Foundations of Computer Science* (1994).
23. Shor, P. W. Scheme for reducing decoherence in quantum computer memory. *Phys. Rev. A* **52**, R2493–R2496 (1995).
24. Gyongyosi, L., Imre, S. & Nguyen, H. V. A Survey on Quantum Channel Capacities. *IEEE Communications Surveys and Tutorials* **99**, 1, https://doi.org/10.1109/COMST.2017.2786748 (2018).

25. Biamonte, J. *et al*. Quantum Machine Learning. *Nature* **549**, 195–202 (2017).
26. Lloyd, S., Mohseni, M. & Rebentrost, P. Quantum algorithms for supervised and unsupervised machine learning, *arXiv:1307.0411v2* (2013).
27. Lloyd, S., Mohseni, M. & Rebentrost, P. Quantum principal component analysis. *Nature Physics* **10**, 631 (2014).
28. Monz, T. *et al*. Realization of a scalable Shor algorithm. *Science* **351**, 1068–1070 (2016).
29. Barends, R. *et al*. Superconducting quantum circuits at the surface code threshold for fault tolerance. *Nature* **508**, 500–503 (2014).
30. Kielpinski, D., Monroe, C. & Wineland, D. J. Architecture for a large-scale ion-trap quantum computer. *Nature* **417**, 709–711 (2002).
31. Ofek, N. *et al*. Extending the lifetime of a quantum bit with error correction in superconducting circuits. *Nature* **536**, 441–445 (2016).
32. Rebentrost, P., Mohseni, M. & Lloyd, S. Quantum Support Vector Machine for Big Data Classification. *Phys. Rev. Lett*. **113** (2014).
33. Lloyd, S. The Universe as Quantum Computer, *A Computable Universe: Understanding and exploring Nature as computation*, Zenil, H. ed., World Scientific, Singapore, 2012, *arXiv:1312.4455v1* (2013).
34. LeCun, Y., Bengio, Y. & Hinton, G. Deep Learning. *Nature* **521**, 436–444 (2014).
35. Schuld, M., Sinayskiy, I. & Petruccione, F. An introduction to quantum machine learning. *Contemporary Physics* **56**, pp. 172-185. *arXiv: 1409.3097* (2015).
36. Imre, S. & Gyongyosi, L. *Advanced Quantum Communications - An Engineering Approach*. Wiley-IEEE Press (New Jersey, USA) (2012).
37. Petz, D. *Quantum Information Theory and Quantum Statistics*, Springer-Verlag, Heidelberg, Hiv: **6** (2008).
38. Bacsardi, L. On the Way to Quantum-Based Satellite Communication. *IEEE Comm. Mag.* **51**(08), 50–55 (2013).
39. Van Meter, R. *Architecture of a Quantum Multicomputer Optimized for Shor's Factoring Algorithm*, Ph.D Dissertation, Keio University, *arXiv:quant-ph/0607065v1* (2006).
40. Brandao, F. G. S. L., Broughton, M., Farhi, E., Gutmann, S. & Neven, H. For Fixed Control Parameters the Quantum Approximate Optimization Algorithm's Objective Function Value Concentrates for Typical Instances, *arXiv:1812.04170* (2018).
41. Zhou, L., Wang, S.-T., Choi, S., Pichler, H. & Lukin, M. D. Quantum Approximate Optimization Algorithm: Performance, Mechanism, and Implementation on Near-Term Devices, arXiv:1812.01041 (2018).
42. Lechner, W. Quantum Approximate Optimization with Parallelizable Gates, *arXiv:1802.01157v2* (2018).
43. Crooks, G. E. Performance of the Quantum Approximate Optimization Algorithm on the Maximum Cut Problem, *arXiv:1811.08419* (2018).
44. Ho, W. W., Jonay, C. & Hsieh, T. H. Ultrafast State Preparation via the Quantum Approximate Optimization Algorithm with Long Range Interactions, *arXiv:1810.04817* (2018).
45. Song, C. *et al*. 10-Qubit Entanglement and Parallel Logic Operations with a Superconducting Circuit. *Physical Review Letters* **119**(no. 18), 180511 (2017).
46. Brown, K. A. & Roser, T. Towards storage rings as quantum computers. *Phys. Rev. Accel. Beams* **23**, 054701 (2020).
47. Gyongyosi, L. & Imre, S. Unsupervised Machine Learning Control of Quantum Gates in Gate-Model Quantum Computers, *Proceedings of the Frontiers in Optics 2018* (FiO 2018), Optical Society of America (OSA), 16-20 Sept. 2018, Washington, D.C., USA, https://doi.org/10.1364/FIO.2018.FTh1B.3 (2018).
48. Chou, C. W. *et al*. Measurement-induced entanglement for excitation stored in remote atomic ensembles. *Nature* **438**, 828–832 (2005).
49. Nemoto, K. & Munro, W. J. Nearly deterministic linear optical controlled-NOT gate. *Physical Review Letters* **93**, 250502 (2004).
50. Munro, W., Nemoto, K. & Spiller, T. Weak nonlinearities: a new route to optical quantum computation. *New Journal of Physics* **7**, 137 (2005).
51. Spiller, T. P. *et al*. Quantum computation by communication. *New Journal of Physics* **8**, 30 (2006).
52. Lloyd, S. *et al*. Infrastructure for the quantum Internet. *ACM SIGCOMM Computer Communication Review* **34**, 9–20 (2004).
53. Goodfellow, I., Bengio, Y. & Courville, A. *Deep Learning*. MIT Press. Cambridge, MA (2016).
54. Lloyd, S., Garnerone, S. & Zanardi, P. Quantum algorithms for topological and geometric analysis of data. *Nat. Commun*., **7**, arXiv:1408.3106 (2016).
55. Debnath, S. *et al*. Demonstration of a small programmable quantum computer with atomic qubits. *Nature* **536**, 63–66 (2016).
56. Pirandola, S. & Braunstein, S. L. Unite to build a quantum internet. *Nature* **532**, 169–171 (2016).
57. Pirandola, S. End-to-end capacities of a quantum communication network. *Commun. Phys.* **2**, 51 (2019).
58. Wehner, S., Elkouss, D. & Hanson, R. Quantum internet: A vision for the road ahead. *Science* **362**, 6412 (2018).
59. Pirandola, S., Laurenza, R., Ottaviani, C. & Banchi, L. Fundamental limits of repeaterless quantum communications. *Nature Communications* **8**, 15043, https://doi.org/10.1038/ncomms15043 (2017).
60. Pirandola, S. *et al*. Theory of channel simulation and bounds for private communication. *Quantum Sci. Technol.* **3**, 035009 (2018).
61. Pirandola, S. Bounds for multi-end communication over quantum networks. *Quantum Sci. Technol.* **4**, 045006 (2019).
62. Pirandola, S. Capacities of repeater-assisted quantum communications, *arXiv:1601.00966* (2016).
63. Pirandola, S. *et al*. Advances in Quantum Cryptography, *arXiv:1906.01645* (2019).
64. Laurenza, R. & Pirandola, S. General bounds for sender-receiver capacities in multipoint quantum communications. *Phys. Rev. A* **96**, 032318 (2017).
65. Kimble, H. J. The quantum Internet. *Nature* **453**, 1023–1030 (2008).
66. Van Meter, R. & Devitt, S. J. Local and Distributed Quantum Computation. *IEEE Computer* **49**(9), 31–42 (2016).
67. Gyongyosi, L. & Imre, S. Optimizing High-Efficiency Quantum Memory with Quantum Machine Learning for Near-Term Quantum Devices, *Scientific Reports*, https://doi.org/10.1038/s41598-019-56689-0 (2019).
68. Gyongyosi, L. & Imre, S. Theory of Noise-Scaled Stability Bounds and Entanglement Rate Maximization in the Quantum Internet, *Scientific Reports*, https://doi.org/10.1038/s41598-020-58200-6 (2020).
69. Gyongyosi, L. Services for the Quantum Internet, *DSc Dissertation*, Hungarian Academy of Sciences (MTA) (2020).
70. Gyongyosi, L. & Imre, S. Entanglement Access Control for the Quantum Internet, *Quantum Information Processing*, Springer Nature, https://doi.org/10.1007/s11128-019-2226-5 (2019).
71. Gyongyosi, L. & Imre, S. Opportunistic Entanglement Distribution for the Quantum Internet, *Scientific Reports*, https://doi.org/10.1038/s41598-019-38495-w (2019).
72. Gyongyosi, L. & Imre, S. Dense Quantum Measurement Theory, *Scientific Reports*, https://doi.org/10.1038/s41598-019-43250-2 (2019).
73. Gyongyosi, L. & Imre, S. Training Optimization for Gate-Model Quantum Neural Networks, *Scientific Reports*, https://doi.org/10.1038/s41598-019-48892-w (2019).
74. Gyongyosi, L. & Imre, S. State Stabilization for Gate-Model Quantum Computers, *Quantum Information Processing*, Springer Nature, https://doi.org/10.1007/s11128-019-2397-0 (2019).
75. Gyongyosi, L. & Imre, S. Quantum Circuit Design for Objective Function Maximization in Gate-Model Quantum Computers, *Quantum Information Processing*, https://doi.org/10.1007/s11128-019-2326-2 (2019).
76. Gyongyosi, L. & Imre, S. Multilayer Optimization for the Quantum Internet, *Scientific Reports*, https://doi.org/10.1038/s41598-018-30957-x (2018).

77. Gyongyosi, L. & Imre, S. Entanglement Availability Differentiation Service for the Quantum Internet, *Scientific Reports*, https://doi.org/10.1038/s41598-018-28801-3, https://www.nature.com/articles/s41598-018-28801-3 (2018).

78. Gyongyosi, L. & Imre, S. Entanglement-Gradient Routing for Quantum Networks, *Scientific Reports*, https://doi.org/10.1038/s41598-017-14394-w, https://www.nature.com/articles/s41598-017-14394-w (2017).

79. Gyongyosi, L. & Imre, S. Decentralized Base-Graph Routing for the Quantum Internet, *Physical Review A*, https://doi.org/10.1103/PhysRevA.98.022310 (2018).

80. Chakraborty, K., Rozpedeky, F., Dahlbergz, A. & Wehner, S. Distributed Routing in a Quantum Internet, *arXiv:1907.11630v1* (2019).

81. Khatri, S., Matyas, C. T., Siddiqui, A. U. & Dowling, J. P. Practical figures of merit and thresholds for entanglement distribution in quantum networks. *Phys. Rev. Research* **1**, 023032 (2019).

82. Kozlowski, W. & Wehner, S. Towards Large-Scale Quantum Networks, *Proc. of the Sixth Annual ACM International Conference on Nanoscale Computing and Communication*, Dublin, Ireland, *arXiv*:1909.08396 (2019).

83. Pathumsoot, P. *et al.* Modeling of Measurement-based Quantum Network Coding on IBMQ Devices, *Phys. Rev. A* **101**, 052301 (2020).

84. Pal, S., Batra, P., Paterek, T. & Mahesh, T. S. Experimental localisation of quantum entanglement through monitored classical mediator, *arXiv:1909.11030v1* (2019).

85. Miguel-Ramiro, J. & Dur, W. Delocalized information in quantum networks, *New J. Phys*, https://doi.org/10.1088/1367-2630/ab784d (2020).

86. Pirker, A. & Dur, W. A quantum network stack and protocols for reliable entanglement-based networks, *arXiv:1810.03556v1* (2018).

87. Shannon, K., Towe, E. & Tonguz, O. On the Use of Quantum Entanglement in Secure Communications: A Survey, *arXiv:2003.07907* (2020).

88. Amoretti, M. & Carretta, S. Entanglement Verification in Quantum Networks with Tampered Nodes, *IEEE Journal on Selected Areas in Communications*, https://doi.org/10.1109/JSAC.2020.2967955 (2020).

89. Cao, Y. *et al.* Multi-Tenant Provisioning for Quantum Key Distribution Networks with Heuristics and Reinforcement Learning: A Comparative Study, *IEEE Transactions on Network and Service Management*, https://doi.org/10.1109/TNSM.2020.2964003 (2020).

90. Cao, Y. *et al.* Key as a Service (KaaS) over Quantum Key Distribution (QKD)-Integrated Optical Networks, *IEEE Comm. Mag.*, https://doi.org/10.1109/MCOM.2019.1701375 (2019).

91. Liu, Y. Preliminary Study of Connectivity for Quantum Key Distribution Network, *arXiv:2004.11374v1* (2020).

92. Sun, F. Performance analysis of quantum channels, *Quantum Eng.* e35, https://doi.org/10.1002/que2.35 (2020).

93. Chai, G. *et al.* Blind channel estimation for continuous-variable quantum key distribution, *Quantum Eng.* e37, https://doi.org/10.1002/que2.37 (2020).

94. Krisnanda, T. *et al.* Probing quantum features of photosynthetic organisms. *npj Quantum Inf.* **4**, 60 (2018).

95. Krisnanda, T. *et al.* Revealing Nonclassicality of Inaccessible Objects. *Phys. Rev. Lett.* **119**, 120402 (2017).

96. Krisnanda, T. *et al.* Observable quantum entanglement due to gravity. *npj Quantum Inf.* **6**, 12 (2020).

97. Krisnanda, T. *et al.* Detecting nondecomposability of time evolution via extreme gain of correlations. *Phys. Rev. A* **98**, 052321 (2018).

98. Caleffi, M. End-to-End Entanglement Rate: Toward a Quantum Route Metric, 2017 *IEEE Globecom*, https://doi.org/10.1109/GLOCOMW.2017.8269080 (2018).

99. Caleffi, M. Optimal Routing for Quantum Networks, *IEEE Access*, Vol 5, https://doi.org/10.1109/ACCESS.2017.2763325 (2017).

100. Caleffi, M., Cacciapuoti, A. S. & Bianchi, G. Quantum Internet: from Communication to Distributed Computing, *aXiv:1805.04360* (2018).

101. Castelvecchi, D. The quantum internet has arrived, *Nature*, News and Comment, https://www.nature.com/articles/d41586-018-01835-3 (2018).

102. Cacciapuoti, A. S., *et al* Quantum Internet: Networking Challenges in Distributed Quantum Computing, *arXiv:1810.08421* (2018).

103. Cuomo, D., Caleffi, M. & Cacciapuoti, A. S. Towards a Distributed Quantum Computing Ecosystem, *arXiv:2002.11808v1* (2020).

104. Miguel-Ramiro, J., Pirker, A. & Dur, W. Genuine quantum networks: superposed tasks and addressing. *arXiv:2005.00020v1* (2020).

105. Amer, O., Krawec, W. O. & Wang, B. Efficient Routing for Quantum Key Distribution Networks. *arXiv:2005.12404* (2020).

106. Rozpedek, F. *et al.* Optimizing practical entanglement distillation. *Phys. Rev. A* **97**, 062333 (2018).

107. Humphreys, P. *et al.* Deterministic delivery of remote entanglement on a quantum network, *Nature* **558** (2018).

108. Liao, S.-K. *et al.* Satellite-to-ground quantum key distribution. *Nature* **549**, 43–47 (2017).

109. Ren, J.-G. *et al.* Ground-to-satellite quantum teleportation. *Nature* **549**, 70–73 (2017).

110. Hensen, B. *et al.* Loophole-free Bell inequality violation using electron spins separated by 1.3 kilometres, *Nature* **526** (2015).

111. Hucul, D. *et al.* Modular entanglement of atomic qubits using photons and phonons, *Nature Physics* **11**(1) (2015).

112. Noelleke, C. *et al.* Efficient Teleportation Between Remote Single-Atom Quantum Memories. *Physical Review Letters* **110**, 140403 (2013).

113. Sangouard, N. *et al.* Quantum repeaters based on atomic ensembles and linear optics. *Reviews of Modern Physics* **83**, 33 (2011).

114. Quantum Internet Research Group (QIRG), web: https://datatracker.ietf.org/rg/qirg/about/ (2018).

115. Duriez, T., Brunton, S. L. & Noack, B. R. *Machine Learning Control: Taming Nonlinear Dynamics and Turbulence*, ISSN 0926-5112 ISSN 2215-0056 (electronic), Springer (2017).

116. Noack, B. R. & Niven, R. K. Maximum-entropy closure for a Galerkin system of an incompressible periodic wake. *J. Fluid Mech.* **700**, 187–213 (2012).

117. Low, K. R. *et al.* Noise source identification and control in a Mach 0.6 turbulent jet with simultaneous time resolved PIV, pressure and acoustic measurements. *Exp. Fluids* **54**(4), 1–17 (2013).

118. Zahedinejad, E., Ghosh, J. & Sanders, B. C. Designing high-fidelity single-shot three-qubit gates: A machine-learning approach. *Physics Review Applied* **6**, 054005 (2016).

119. Zahedinejad, E., Schirmer, S. & Sanders, B. C. Evolutionary algorithms for hard quantum control. *Physics Review A* **90**(no. 3), 032310 (2014).

120. Wu, C., Qi, B., Chen, C. & Dong, D. Robust learning control design for quantum unitary transformations, *IEEE Transactions on Cybernetics* (2018).

121. Bukov, M. *et al.* Reinforcement Learning in Different Phases of Quantum Control. *Phys. Rev. X* **8**, 031086 (2018).

122. Dong, D. *et al.* Learning robust pulses for generating universal quantum gates. *Scientific Reports* **6**, 36090 (2016).

123. Farhi, E., Goldstone, J., Gutmann, S. & Sipser, M. Quantum computation by adiabatic evolution. *Technical Report MIT-CTP-2936*, MIT, arXiv:quant-ph/0001106 (2000).

124. Kadowaki, T. & Nishimori, H. Quantum annealing in the transverse Ising model. *Phys. Rev. E* **58**, 5355–5363, arXiv:cond-mat/9804280 (1998).

125. Khaneja, N. *et al.* Optimal control of coupled spin dynamics: design of NMR pulse sequences by gradient ascent algorithms. *Journal of magnetic resonance* **172.2**, 296–305 (2005).

126. Farhi, E. & Harrow, A. W. Quantum Supremacy through the Quantum Approximate Optimization Algorithm, *arXiv:1602.07674* (2016).

127. Farhi, E., Kimmel, S. & Temme, K. A Quantum Version of Schoning's Algorithm Applied to Quantum 2-SAT, *arXiv:1603.06985* (2016).
128. Sax, I. *et al.* Approximate Approximation on a Quantum Annealer, *arXiv:2004.09267* (2020).
129. Li, R. *et al.* Approximate Quantum Adders with Genetic Algorithms: An IBM Quantum Experience. *Quantum Measurements and Quantum Metrology* **4**, 1 (2017).
130. Gyongyosi, L. & Imre, S. A Survey on Quantum Computing Technology, *Computer Science Review*, Elsevier, https://doi.org/10.1016/j.cosrev.2018.11.002, ISSN: 1574-0137 (2018).
131. Armen, M. A., Au, J. K., Stockton, J. K., Doherty, A. C. & Mabuchi, H. Adaptive homodyne measurement of optical phase. *Physical Review Letters* **89**, 133602 (2002).

Acknowledgements

Author contributions

L.G.Y. designed the protocol, wrote the manuscript, and analyzed the results.

Competing interests

The author declares no competing interests.

Additional information

Supplementary information is available for this paper at https://doi.org/10.1038/s41598-020-67018-1.

Correspondence and requests for materials should be addressed to L.GY.

Reprints and permissions information is available at www.nature.com/reprints.

Publisher's note Springer Nature remains neutral with regard to jurisdictional claims in published maps and institutional affiliations.